J Mater Sci (2019) 54:4984–4996

Materials for life sciences

The strengthening of woven jute fiber/polylactide biocomposite without loss of ductility using rigid core–soft shell nanoparticles

Hailing He[1,2], Tong Earn Tay[2], Zhenqing Wang[1,*], and Zhiwei Duan[1]

[1] College of Aerospace and Civil Engineering, Harbin Engineering University, Harbin 150001, China
[2] Department of Mechanical Engineering, National University of Singapore, Singapore 117576, Singapore

Received: 10 October 2018
Accepted: 26 November 2018
Published online: 3 December 2018

ABSTRACT

Some efforts have been made to strengthen the environment friendly natural fiber-reinforced polylactide composite (NFPC), but common approaches impair its ductility. This paper successfully synthesized the rigid-soft core–shell nanoparticles which are feasible to simultaneously improve the strength and toughness of NFPC. The core–shell structure was molecularly designed to act the nano-silica and poly (butyl acrylate) rubber as rigid inner core and soft outer shell, respectively. Furthermore, the devised active functional groups at the end of core–shell filler also interact with polylactide (PLA) matrix to form strong interface. The effect of core–shell nanoparticle on crystalline, thermal and mechanical properties of NFPC was investigated. The results showed that the core–shell nanofiller can facilitate to form the more complete crystalline grain of PLA matrix and the thermal stability improvement of NFPC. More attractively, the addition of the rigid-soft core–shell nanoparticle enhanced the strength and stiffness of NFPC without sacrificing its elongation at break. Finally, the toughness improvement mechanisms and synergistic effect of core–shell nanoparticles were illustrated via field emission scanning electron microscope. It indicates that the micro-cracks, shear band and fibration of the matrix induced by the core–shell filler are the main causes of toughness improvement.

Introduction

In recent years, the natural fiber composite (NFC) has been applied in automotive industry, building construction and sports accessories due to its advantages compared to the synthetic fiber composite, such as environment friendliness, sustainability, low cost, lightweight and high specific strength and stiffness [1–3]. For further to achieve the full biodegradability and reduce petroleum consumption, using the biodegradable polymers as the matrix of the NFC is an excellent choice. Polylactide, which is produced

Address correspondence to E-mail: wangzhenqing@hrbeu.edu.cn

https://doi.org/10.1007/s10853-018-03206-9

from renewable agricultural raw materials, is the most promising biodegradable polymer due to its high strength, stiffness, transparency and commercial production [4]. Therefore, many investigations have been conducted on natural fiber-reinforced polylactide composite [5–7], while the inferior mechanical properties of these NFPC limit their more extensive industrial applications. So some strategies have been developed, for instance, improving the interfacial adhesion between natural fiber and PLA matrix [8, 9]. Huda et al. [10] used the alkali, silane and alkali followed by silane to treat the kenaf fiber, respectively. They found that the alkali followed by silane-treated fiber-reinforced composite showed more superior flexural strength and storage modulus due to the improved interfacial compatibility between the hydrophilic natural fiber and hydrophobic PLA matrix. Except for the fiber surface treatment, the processing condition has also been ameliorated to enhance the performance of NFPC [11]. For example, Plackett et al. [12] investigated the effect of heating temperature and time of compression molding on performances of NFPC. They concluded that the tensile strength of NFPC prepared at 210 °C (3 min) increased 38% compared to that of NFPC prepared at 180 °C (10 min) resulting from the adequate impregnation.

In addition to the optimization of interfacial adhesion and processing condition, the modification of matrix is also an efficient strategy to improve the properties of NFPC. However, there are only a few publications in this regard. Kumar et al. [13] added the montmorillonite clay into PLA matrix to investigate its effect on flax fabric-reinforced composite. The results showed that the Young's modulus of the hybrid NFPC increased remarkably, but its tensile strength increased slightly or even decreased, and the elongation at break declined seriously. This may be attributed to the weakened interfacial adhesion of modifier/matrix and the higher stiffness of montmorillonite clay compared to the PLA resin. Noticeably, a designed molecularly core–shell nanoparticle which is comprised of both rigid and flexible segments was recently used to modify the polymer system [14]. Meanwhile, the active functional groups at the end of nanofiller were feasible to enhance the interfacial interaction of filler/matrix. As a result, the incorporation of this core–shell modifier improved the strength and toughness of thermoset polymer simultaneously. Nevertheless, to our knowledge, there has not yet been reported that this devised core–shell structure is applied to enhance the performance of natural fiber-reinforced biodegradable composite. The synergistic effect between covalently bonded rigid core and soft shell of this core–shell structure will provide the strength increment of natural fiber-reinforced composite while maintaining its ductility.

In this paper, this rigid-soft core–shell nanoparticle was introduced into the PLA matrix to improve the mechanical properties of woven jute fiber-reinforced PLA composite. The nano-silica and poly (butyl acrylate) were designed as the rigid inner core and rubbery outer shell of core–shell filler, respectively. The effect of core–shell nanoparticle on crystalline and thermal properties of NFPC were investigated by the X-ray diffraction (WAXD), differential scanning calorimetry (DSC) and thermogravimetric analysis (TGA). Furthermore, the contribution of core–shell nanofiller to the strength, stiffness and ductility of NFPC was also explored by the tensile and flexural tests. Subsequently, the mechanism of mechanical enhancement and synergistic effect of designed core–shell nanoparticle were also analyzed.

Materials and methods

Materials

Polylactide (3051D, 96.5% of L-lactide, M_w:160 kDa, polydispersity:1.7) was supplied by Natureworks. The woven jute fiber used in this work was purchased from Zhenjiang, China. The jute fabric is plain weave, and its average weight is about 280 g/m^2. The tensile strength and density of jute fiber are 340 MPa and 1.21 g/cm^3, respectively. Nano-silica (Aerosil 380, raw particle diameter of 7 nm) white powder with a specific surface area of 380 ± 30 m^2/g was attained from Evonik. *n*-Butyl acrylate (*n*-BA, > 99%), 3-aminopropyltriethoxysilane (APTES, > 99%) and other chemicals were purchased from Aldrich Chemical Reagents Co.

Synthesis of core–shell nanoparticles

The AGET ATRP (activators generated by electron transfer, atom-transfer radical polymerization) was utilized to synthesize the silica-rubber core–shell nanoparticle [15, 16]. As shown in Fig. 1, the amino-

functionalized silica nanoparticles (SiO_2–NH_2) was first prepared by the silanization reaction of abundant hydroxyl on the silica surface with silane coupling agent (APTES) for 16 h at 95 °C in an oil bath. Subsequently, to realize the polymerization grafting of butyl acrylate (BA) monomer, the initiator was immobilized at the surface of silanized silica to obtain the SiO_2–Br. The 2-bromoisobutyryl bromide (BiB) was added dropwise to mixed solution of silanized silica, trimethylamine and toluene. The immobilization reaction was processed for 3 h at 0 °C and 12 h at room temperature. Then, the iron-mediated AGET ATRP technique was applied to synthesize the SiO_2–PBA core–shell nanoparticle. In the presence of initiator, graft polymerization of the butyl acrylate (BA) rubber shell was initiated on the nano-silica surface using the $FeCl_3$/triphenylphosphine (PPh_3) as catalyst complex and ascorbic acid (VC) as reducing agent. The polymerization procedure was carried on for 8 h at 90 °C. The obtained rigid core–soft shell nanoparticle with end bromine group was denoted as SiO_2–PBA–Br. Furthermore, to promote the covalent bonding between core–shell filler and polylactide matrix, the 'click' reaction was used to transfer the end bromine group of PBA shell to the active amine group [14]. The SiO_2–PBA–Br core–shell particle, trimethylamine and cysteamine were dissolved in tetrahydrofuran and stirred overnight at room temperature. The obtained core–shell nanoparticle with the terminal amino group was designated as SiO_2–PBA–NH_2.

Preparation of woven jute fiber-reinforced PLA composite

To improve the interfacial adhesion between hydrophilic jute fiber and hydrophobic PLA, the surface treatment of natural jute fiber was implemented firstly. The jute fibers were immersed in sodium hydroxide solution (5% w/v) for 2 h at room temperature and then were washed with distilled water until pH of 7. After washing, the fibers were dried in air for 12 h followed by dried in vacuum oven at 80 °C for 6 h. The alkali-treated fibers were immersed in the mixture of water/ethanol (40:60 w/w) with 5 wt% APTES (weight percentage compared to the fiber) for 3 h. Then, the fibers were washed and dried in air for 12 h followed by dried in vacuum oven at 80 °C for 6 h.

The composite laminates containing 40 wt% woven jute fiber were fabricated by hot pressing of prepregs, as shown in Fig. 2. Firstly, the specific weight of dried PLA pellet was dissolved in the dichloromethane. The 1 wt% core–shell nanoparticle (SiO_2–PBA–NH_2) was dispersed in ethanol and sonicated for 30 min. Secondly, the nanoparticle solution was mixed with the PLA resin and the mixture was stirred to homogeneity. The obtained modified matrix was poured onto the woven jute fiber to prepare the prepregs. After the solvent volatilizing, the obtained prepregs were dried in the vacuum at 60 °C. Before hot pressing, the steel mold was heated to 160 °C, and subsequently, the dried prepregs were stacked in the

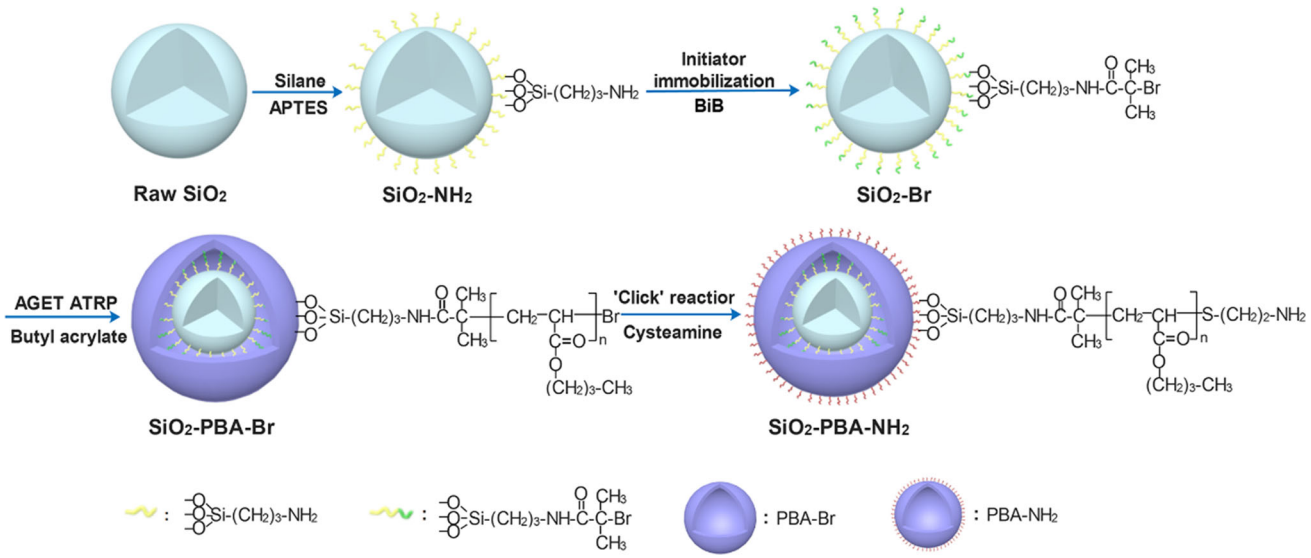

Figure 1 Synthesis schematic of silica-rubber core–shell nanoparticle.

groove of the steel mold. Then, a thick steel sheet was covered on above steel mold. Finally, the fabric stacks were hot compressed at 160 °C for 20 min by the hot-press machine. The obtained sample is denoted as NFPC/SiO_2–PBA–NH_2. The NFPC represents the jute fiber-reinforced unmodified-PLA composite. For comparison, the nanoparticles of SiO_2 and SiO_2–NH_2 were also used to modify the PLA matrix, and the as-prepared jute fiber-reinforced nanocomposites are designated as NFPC/SiO_2 and NFPC/SiO_2–NH_2.

Materials characterization

The characterization of core–shell nanoparticle was analyzed by the Fourier transform infrared spectroscopy (FTIR). The morphology and size of the core–shell nanoparticles were investigated using the transmission electron microscope (TEM) (JEOL2100F) operated at 200 kV.

The crystalline, thermal, mechanical properties and morphology of jute-reinforced PLA composites were also characterized. Wide-angle X-ray diffraction (WAXD) was performed on a Smartlab9 diffractometer under a voltage of 40 kV using the Cu Kα radiation. The differential scanning calorimetry (DSC) measurement was taken under N_2 using NETZSCH DSC 200F3. The samples were first heated from 25 to 200 °C by the heating rate of 20 °C/min and held at the 200 °C for 5 min to release the thermal history. Subsequently, the samples were cooled down to the 0 °C at the rate of 20 °C/min quickly and kept for 2 min. Then, the samples were heated to 200 °C again at the rate of 10 °C/min. During this process, the DSC thermograms were recorded, and the glass transition temperature (T_g) and melting temperature (T_m) can be determined. Thermogravimetric analysis (TGA) was performed on a thermogravimetric analyzer of NETZSCH STA 449F3. About 8 mg of samples were heated from 30 to 600 °C at a rate of 10 °C/min in nitrogen atmosphere. Thermal degradation temperature of jute fiber, PLA and composites were evaluated as temperature corresponding to the maximum rate of the weight loss. The tensile properties of fiber-reinforced laminate were obtained according to the ASTM Standard D3039 using an Instron 5500R testing machine at a crosshead speed of 2 mm/min. The flexural properties were measured according to ASTM D790 using Zwick/Roell Z010 machine. The fracture surface morphologies of the tensile samples were observed using a scanning electron microscopy (SEM) (JEOL JSM 6390) at an accelerating voltage of 10 kV. Before examination, a thin layer of gold was sputter-coated onto the specimen surfaces to avoid electrostatic charging. Dispersion of core–shell nanoparticles in PLA matrix and detailed fracture morphology of PLA/SiO_2–PBA–NH_2 nanocomposite were examined using the field emission scanning electron microscope (FE-SEM, ZEISS) operated at 15 kV.

Results and discussion

Characterization of core–shell nanoparticle

The FTIR can be used to verify the graft polymerization of the butyl acrylate on nano-silica surface. From Fig. 3, the peaks at 806 and 1055 cm^{-1} are the

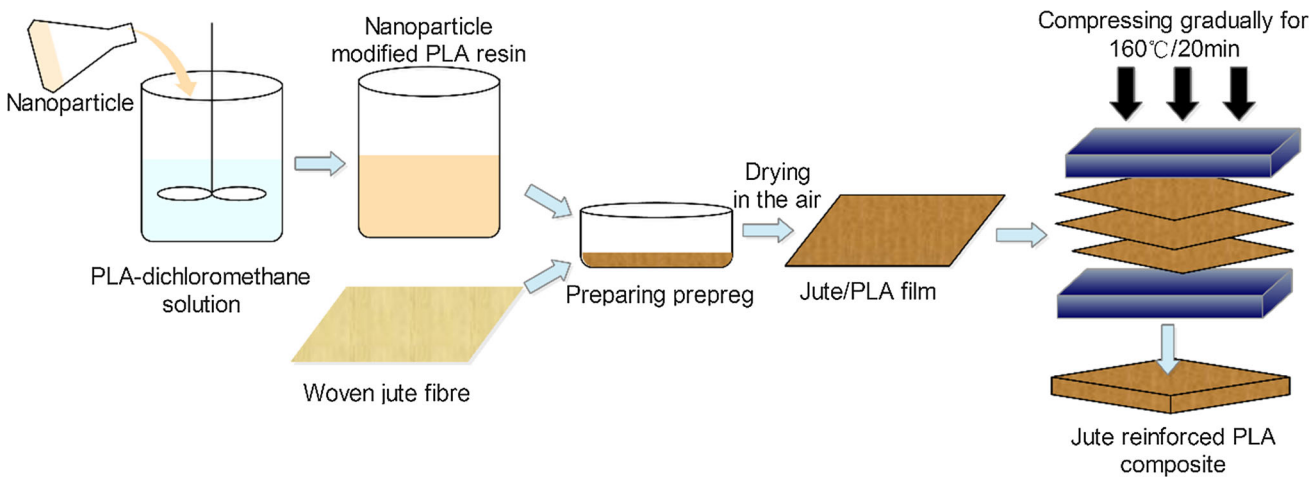

Figure 2 Fabrication of jute-reinforced PLA laminated composite.

result of Si–O–Si and Si–O stretching vibration from the silica nanoparticle, respectively. Compared with the FTIR spectrum of SiO_2, the new peaks at 1396 cm^{-1} from the C–N stretching vibration and at 1650 cm^{-1} from the C=O of acrylamide were presented in the spectrum of SiO_2–PBA–NH_2, which verified that the 2-bromoisobutyryl bromide was initiated to the silica [17]. The adsorption peak at 1732 cm^{-1} was the characteristic of C=O group from the PBA. Meanwhile, the peaks at 2875 cm^{-1}, 1382 cm^{-1} and 1433 cm^{-1} from the C–H vibration indicated the presence of methyl group. The peak at 2934 and 1469 cm^{-1} was attributed to the C–H stretching and bending vibration of methylene. All of these indicated that the PBA was grafted on the silica surface successfully [16]. The stretching vibration of C–S at 694 cm^{-1} and the bending vibration of NH_2 at 1533 cm^{-1} revealed that the amine groups were bonded to the terminal of rubber shell.

The TEM morphologies of raw SiO_2 and SiO_2–PBA–NH_2 core–shell nanoparticle are shown in Fig. 4. Compared Fig. 4a with b, it is clearly seen that the nanoparticle size becomes larger after surface grafting. The light PBA shell was surrounded on the surface of rigid SiO_2 core. The average diameter of raw SiO_2 is about 11.3 nm. After graft polymerization of butyl acrylate, the average diameter of core–shell nanoparticle is about 19.3 nm. The thickness of rubber shell is about 4 nm.

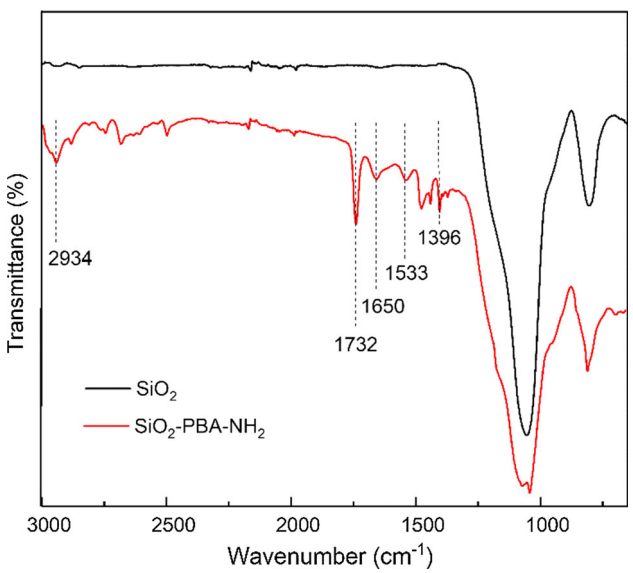

Figure 3 FTIR spectra of SiO_2 and SiO_2–PBA–NH_2 nanoparticle.

Crystalline and thermal properties of NFPC

The crystalline structures of the jute fiber, PLA/jute fiber composite (NFPC) and NFPC/SiO_2–PBA–NH_2 were characterized by the WAXD, as shown in Fig. 5. It can be seen that the jute fiber exhibited a prominent diffraction peak at $2\theta = 22.4°$ corresponding to the (002) lattice plane of cellulose I. Another low-intensity peak presented at $2\theta = 16.4°$ is attributed to its (010) lattice plane [18]. In the PLA/jute fiber composite, a sharp diffraction peak appeared at $2\theta = 16.4°$ compared to the broad peak in the jute fiber, which is corresponded to the (110/200) lattice plane of α-form homocrystallite of PLA. It revealed that the natural jute fiber can promote the crystallization of PLA molecular chain acting as the heterogeneous nucleus [19]. The characteristic of natural fiber to accelerate the crystallization of PLA matrix has also been found in hemp and kenaf fiber/PLA biocomposites [20, 21]. Moreover, the natural fiber can induce the transcrystallinity from their surface in the semicrystalline PLA polymer, especially when the impurities (e.g., wax and pectin) of fiber surface were removed by the chemical treatment [22]. With the core–shell nanoparticle (SiO_2–PBA–NH_2) incorporated, the sharper and higher intensity of aforementioned characteristic peak of PLA ($2\theta = 16.4°$) was obtained in the nanocomposite. Causally, the core–shell filler, acting as a nucleating agent of PLA, promoted the formation of complete crystalline grain. In addition, the as-prepared NFPC/SiO_2–PBA–NH_2 nanocomposite presents an additional peak at $2\theta = 18.9°$ due to the diffraction from (203) lattice plane of α-form crystallite of PLA [23]. These demonstrated that the nanoparticle has an effect of heterogeneous nucleation on the crystallization of PLA matrix. This phenomenon has also been confirmed in the calcium carbonate and layered silicate-reinforced PLA nanocomposite [24, 25].

The DSC heating thermograms of neat PLA and PLA/jute fiber composites are displayed in Fig. 6. It shows that the thermal properties of PLA in the composites remained unaffected by the addition of the jute fiber. The glass transition temperature (T_g) and melting temperature (T_m) of neat PLA and PLA/jute fiber composite were centered at about 60 and 153 °C. It illustrates that the interaction of jute/matrix is not strong to slow down the mobility of molecular china related to the glass transition. The same conclusion was also revealed in the coir fiber-

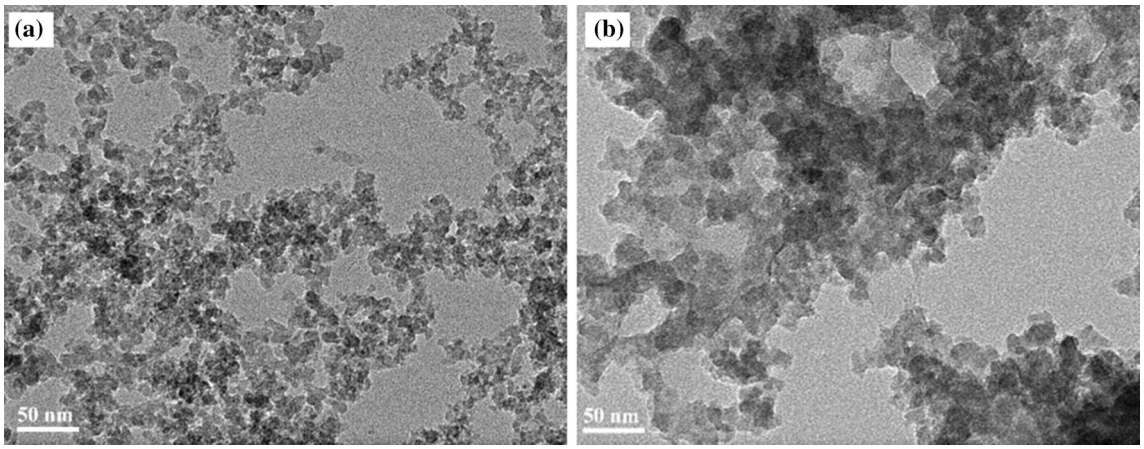

Figure 4 TEM images of **a** raw SiO_2 nanoparticle, **b** SiO_2–PBA–NH_2 core–shell nanoparticle.

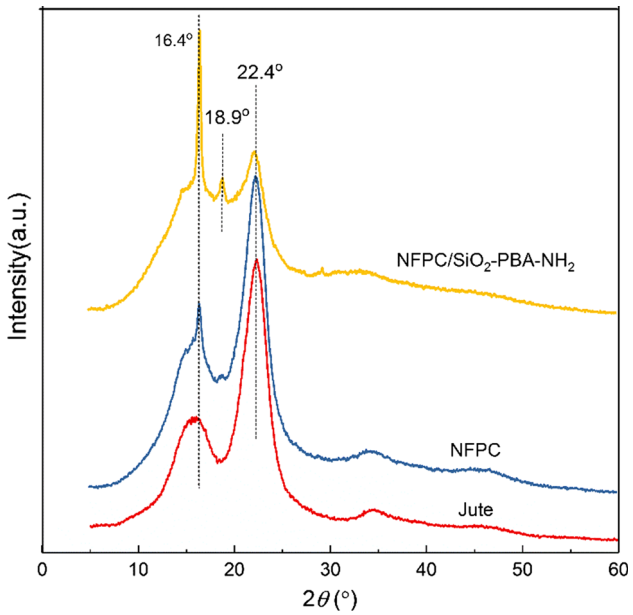

Figure 5 WAXD diffractograms of jute fiber and jute fiber/PLA composites.

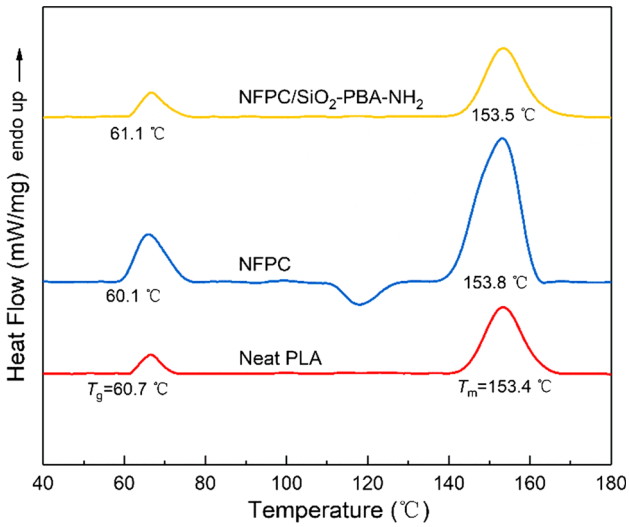

Figure 6 DSC thermogram of neat PLA and jute fiber/PLA composite.

reinforced PLA biocomposite [26]. As the silica-rubber core–shell nanoparticles were introduced into the PLA matrix, the T_g and T_m of nanocomposite almost did not change with considering the experimental deviation, although the rubber within the core–shell filler being added. It is reported that the mobility of polymer chains has a prominent effect on the T_g and T_m of composite [27]. The core–shell nanoparticles used in this study has a strong interfacial bonding with the matrix due to its end active amine group. Therefore, the migration and diffusion of PLA molecular chains near the interacting interface was confined, which contributed to the high thermal stability of core–shell nanofiller-reinforced biocomposite.

The thermal stability of neat PLA, jute fiber and NFPC determined by TGA and derivative thermogravimetric (DTG) are shown in Table 1 and Fig. 7. The temperature (T_d) of maximal thermal degradation rate can be obtained from the peak value of DTG curve. The neat PLA showed a single step thermal degradation at T_d of 358 °C. There were three-stage weight losses in the TGA curve of jute fiber. The first stage (30–100 °C) is attributed to the moisture loss. The second transition (200–300 °C) is related to the decomposition of low molecular weight components of hemi-cellulose. The third weight loss stage (300–400 °C) corresponds to the thermal degradation of cellulose [28]. As shown in Fig. 7b, the T_d of PLA/

jute fiber composite decreased to the 343 °C compared to the neat PLA of 358 °C, which may be attributed to the lower thermal degradation temperature of jute fiber. The observation is in good agreement with the thermal properties of composites reinforced with other natural fibers [26]. As the silica-rubber core–shell nanoparticles were introduced into the PLA matrix, the thermal stability of composite was improved. The initial temperature of thermal degradation and T_d were both increased compared to that of NFPC, which is ascribed to the excellent thermal stability of rigid silica core. Similarly, Siengchin et al. [29] obtained that the incorporation of alumina particles can enhance the thermal resistance of flax/PLA biocomposite at high temperature. Furthermore, the poly (butyl acrylate) (PBA) designed as the outer shell in this study can increase the thermal stability of composite, which has been confirmed by the Qin et al. [30]. This can be explained as that the interaction between poly (butyl acrylate) and polylactide molecular chain improves the entanglement density of PLA matrix.

Mechanical properties

Flexural properties

The flexural stress–strain curves of neat PLA and nanoparticle-modified PLA/jute fiber composites are presented in Fig. 8a. It can be observed that the curve of neat PLA showed a linear evolution, while the PLA/jute fiber composites appeared the initial linear deformation, followed by a nonlinear deformation due to the introduction of jute fiber. The initial linearity indicates the elastic properties of jute/PLA composite. With the applied load increases, the nonlinearity of flexural stress–strain curve appeared due to the beginning of matrix cracking and fiber breaking. The similar phenomena were observed in woven bamboo/PLA biocomposite as well [31]. As shown in Fig. 8a, the NFPC exhibits a significant improvement of flexural properties compared to neat PLA, the flexural strength and modulus increased 37.9 and 101%, respectively. It is resulted from the strong mechanical properties of jute fiber and interfacial adhesion between fiber and matrix. The compatible interface between silanized jute fiber and PLA matrix promoted the stress transfer effectively. Accordingly, little or no fiber pull-out and delamination were observed from the tested specimens.

Furthermore, the nanoparticles applied to modify the PLA resin had a prominent reinforcement to the NFPC. The effects of raw silica (SiO_2), silanized silica (SiO_2–NH_2) and core–shell nanoparticle (SiO_2–PBA–NH_2) on the flexural strength and modulus of NFPC are shown in Fig. 8b. The flexural strength and modulus of NFPC are 87.3 MPa and 4.87 GPa, respectively. In comparison of NFPC, the flexural strength of NFPC/SiO_2–NH_2 composite increased 18.9%. Due to the presence of the terminated amine group on the surface of silica, the SiO_2–NH_2 nanoparticle can be comparatively well dispersed in the matrix to enhance the efficient load transfer between modifier and PLA. Moreover, with incorporation of the SiO_2–PBA–NH_2 core–shell nanofiller, the strength and modulus of NFPC/SiO_2–PBA–NH_2 composite enhanced to 115.3 MPa and 5.33 GPa, respectively, about 32 and 9.4% higher than those of NFPC, simultaneously, increased 11.9 and 7.9% compared to the NFPC/SiO_2–NH_2 composite. This could be attributed to that the core–shell filler with the end-amino group can form the strong interfacial chemical bonding with the PLA matrix via the amidation reaction to reduce the debonding of the nanofiller and promote the load transfer [32, 33]. On the other hand, the soft rubber shell of core–shell filler can also dissipate effectively local stress initiated by the rigid core via the large deformation to reduce the cavitation of nanoparticles. More attractively, due to the strong covalently bonding between the rigid and soft phases, the rigid core can hinder the propagation of the cracks formed by the deformation of rubber shell. The synergistic effect between rigid core and soft shell contributed to the reinforcement of jute/PLA composite without impairing its flexibility.

Table 1 Thermal properties of PLA, fiber and composites

Sample	Temperature (°C)				
	T_5	T_{10}	T_{20}	T_{50}	T_d
Neat PLA	318	329	340	355	358
Jute fiber	239	285	320	360	362
NFPC	273	296	316	341	343
NFPC/SiO_2–PBA–NH_2	279	314	332	352	354

T_5, T_{10}, T_{20} and T_{50} are temperatures of 5%, 10%, 20% and 50% weight loss. T_d is temperature of maximal degradation rate

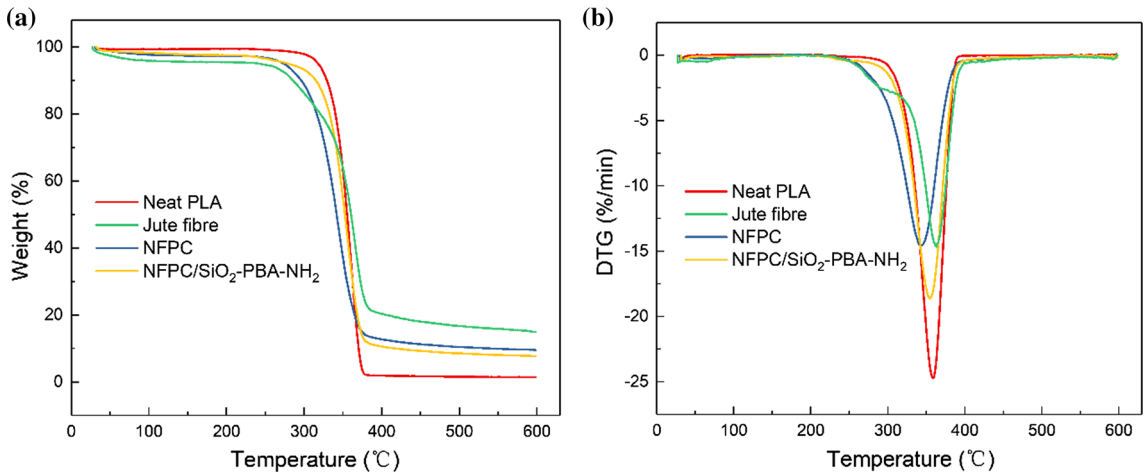

Figure 7 Thermal properties of neat PLA, jute fiber and PLA/fiber composites. **a** TGA thermograms. **b** DTG thermograms.

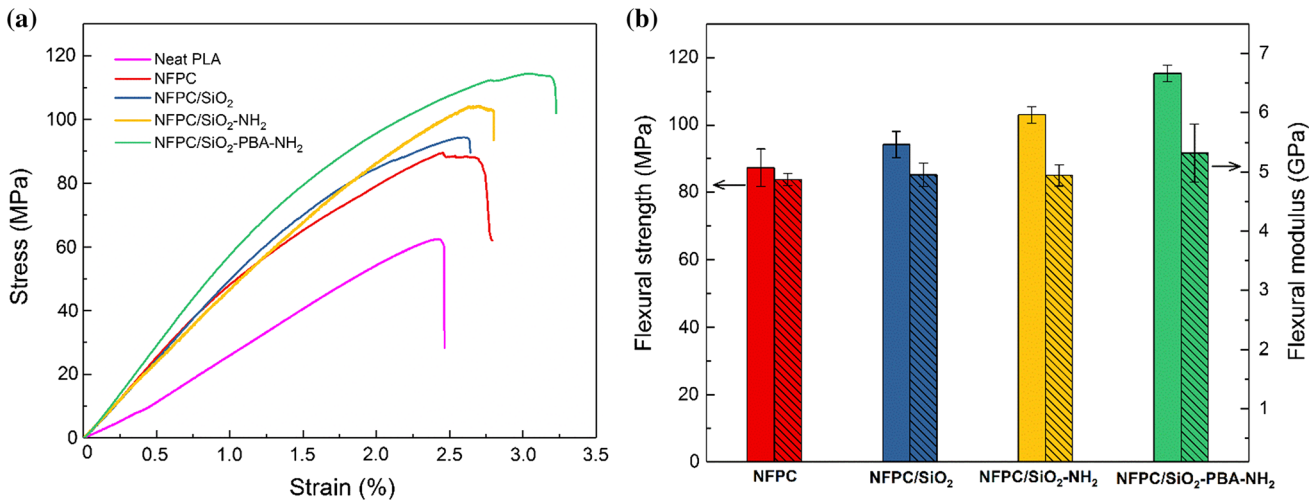

Figure 8 The effect of nanoparticles on flexural properties of PLA/jute fiber composites. **a** Stress–strain curve. **b** Flexural strength and modulus.

Tensile properties

The tensile stress–strain curves of neat PLA and nanoparticle-modified PLA/jute fiber composites are shown in Fig. 9. It is apparent that all samples showed the brittle fracture behaviors, while the nonlinear deformation appeared in the stress–strain curves of PLA/jute fiber composites. The starting of nonlinearity indicated the initial matrix cracking followed by progressive failure of fiber. Moreover, the tensile strength and young's modulus of fiber-reinforced composites increased significantly compared to neat PLA; however, their failure strains declined. This can be attributed to the lower failure strain of the jute fiber compared to that of PLA. From Fig. 9, the tensile strength of NFPC increased to the 52.4 MPa from the 43.1 MPa of neat PLA. The modulus of NFPC was high as 3.14 GPa compared to the PLA of 0.94 GPa, improved 234.0%. This could be attributed to the higher stiffness of jute fiber and the improved fiber wetting when the prepreg technology was applied to prepare the jute/PLA laminate. The similar result about the effect of jute fiber on tensile properties of PLA has been confirmed by Plackett et al. [12].

Figure 10 presents the effects of nano-modifiers on tensile properties of jute fiber-reinforced PLA composites. The toughness was calculated by integrating the tensile stress–strain curves. From Fig. 10, the low content of raw silica had a slight effect on the tensile properties of NFPC owing to the poor interfacial interaction of filler/matrix. With introducing the

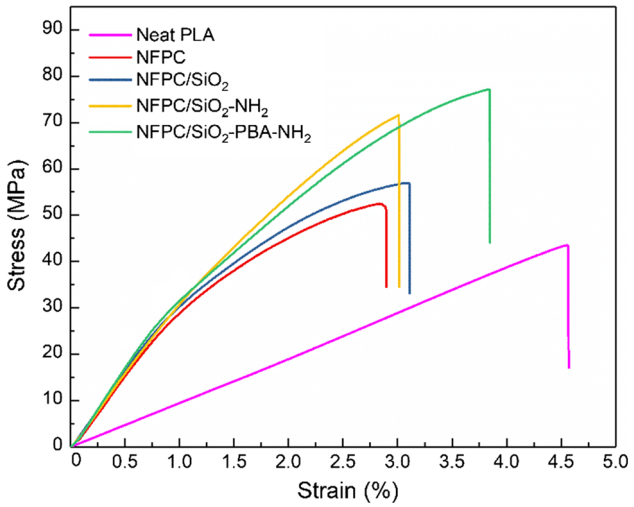

Figure 9 Tensile stress–strain curve of neat PLA and PLA/jute fiber composites.

SiO_2–NH_2 and SiO_2–PBA–NH_2 modifiers to PLA matrix, the modulus of NFPC increased to 3.42 and 3.67 GPa from the 3.14 GPa, respectively. Meanwhile, the tensile strength of NFPC also improved from 52.4–71.9 and 77.5 MPa, respectively. This could be attributed to efficient load transfer between nanofillers and PLA matrix resulting from their perfect interfacial bonding via the amidation reaction. In addition, the nanofillers introduced into the matrix also had the ability to deflect the cracks formed during loading to strengthen the NFPC. Notably, the core–shell nanoparticle also had the excellent toughening effects on the NFPC, demonstrated by the tensile fracture toughness of NFPC/SiO_2–PBA–NH_2 exhibited 97.3% enhancement compared to that of NFPC. Meanwhile, the elongation at break of PLA/jute fiber composite also increased from 2.80 to 3.74%, which may be caused by the great flexibility of PBA rubber shell of core–shell nanoparticle.

To illustrate the toughening mechanism, the fracture surface morphologies of core–shell-reinforced PLA matrix nanocomposite after tensile tests are shown in Fig. 11. The 1 wt% of SiO_2–PBA core–shell nanoparticles are homogeneously distributed in the PLA matrix (labeled by yellow circles in Fig. 11a). The less cavitation/voids occur in the fracture surface, which profits from the desirable interfacial adhesion between core–shell filler and matrix. Being different from the toughening mechanism of pure rubber particle, which the cavitation plays an essential role, the core–shell particle with a superior filler-matrix interaction can also improve the toughness of composite. He et al. [34] concluded that the rubber layer of core–shell particle may initiate the crazes, which is considered to be the key toughening mechanism. Although the crazes did not appear in our fracture surface, as the red arrows shown in Fig. 11a, the flexible rubber layer of core–shell filler facilitates the micro-crack, which is the origin of energy dissipation and thus improves the toughness of nanocomposite. In addition to crack formation, it is hypothesized that the shear band and fibration of matrix induced by the core–shell filler also have the significant toughening effect (as labeled by red circles in Fig. 11b). These shear bands occurred near the core–shell particles, which demonstrates that the rigid-flexible filler can induce the inhomogeneous localized plastic deformation of PLA matrix.

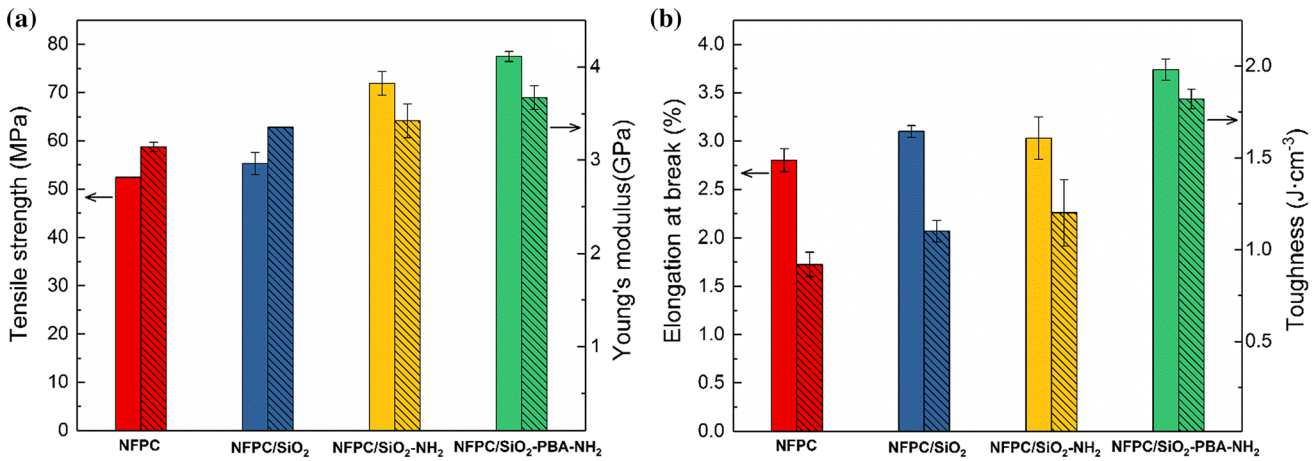

Figure 10 The effect of nanoparticles on tensile properties of PLA/jute fiber composites. **a** Tensile strength and modulus. **b** Elongation at break and toughness.

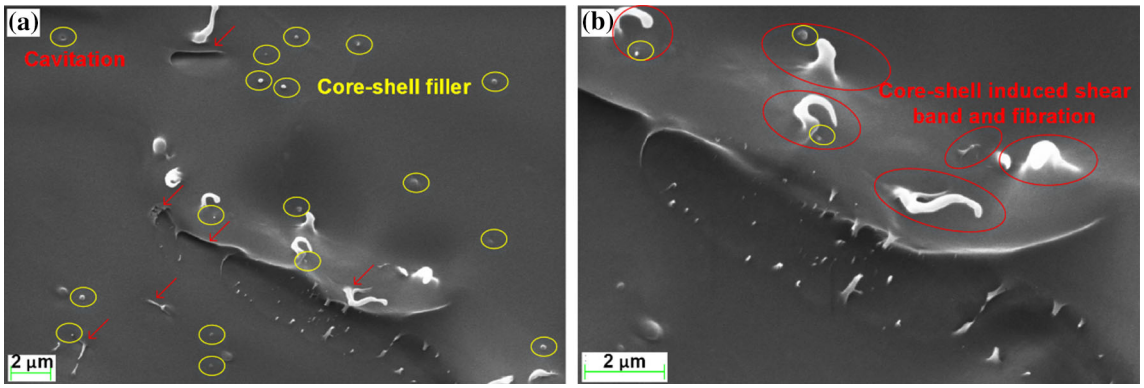

Figure 11 FE-SEM fracture surface morphologies of PLA/SiO_2–PBA–NH_2 nanocomposite.

Moreover, the fibration of matrix could absorb energy remarkably to enhance the toughness of composite.

As expectedly, the core–shell modifier used in this study can contribute to the significant improvement of strength and stiffness of NFPC without sacrifice its toughness and elongation at break. Causally, the synergistic effect of rigid core and flexible shell of core–shell nanoparticle plays a significant role in strengthening and toughening of PLA/jute fiber composite. As shown in Fig. 12, the covalent linkage formed by the grafting polymerization between SiO_2 core and PBA shell can prevent the separation of rigid and rubbery phase. It is resulted in that the two components of rigid and rubbery phase can contribute their respective merits in mechanical properties increment. The rigid SiO_2 core can improve stiffness of matrix, while the flexible PBA shell is related to the enhancement of ductility. The stress transferred to rigid core from the matrix can be relaxed in situ via the deformation of PBA rubber shell, which releases triaxial stress around the core–shell particle further to initiate the shear yielding of PLA matrix. It is considered that the dissipated energy of plastic deformation of matrix is much higher than that of particle debonding [35]. Meanwhile, the micro-cracks formed by the deformation of rubbery phase can be pinned by the chemically bonded rigid SiO_2 core, which makes the paths of cracks deflect or branch. Consequently, the toughness of composite could be improved and the probability of filler debonding or cavitation declines. Further considering the desirable stress transfer between filler and matrix, the strength of composite can be enhanced simultaneously. This synergistic effect of core–shell was also indicated by Yin et al. [36]. They found the thicker shell can prevent the debonding of

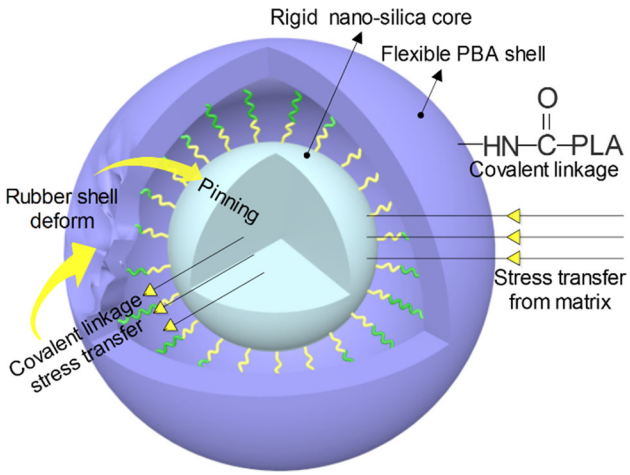

Figure 12 Synergistic effect diagram of core–shell nanoparticle.

core–shell and ensure the stress transfer from matrix to inner core, subsequently, the inner core can avoid the disruption of shell due to the strong interface adhesion of core/shell. As a result, the fibrillation of particle dissipates more fracture energy and thus improves the toughness.

Fracture surface morphologies of PLA/jute fiber composites

To better understand the toughening effect of SiO_2–PBA core–shell nanoparticle on PLA/jute fiber composites, the tensile fracture surfaces of NFPC and NFPC/SiO_2–PBA–NH_2 were observed using SEM as shown in Fig. 13. The fracture surface of PLA matrix of NFPC is smooth (Fig. 13a), and some fractured fiber can also be seen. It is in agreement with the lower elongation at break of NFPC. Nevertheless, the PLA matrix of NFPC/SiO_2–PBA–NH_2 presents a much rougher fracture surface (Fig. 13b), which

demonstrates the localized plastic deformation of PLA matrix can be induced by the core–shell nanoparticle. Figure 13c, d shows the fracture morphologies of PLA matrix permeated through jute fiber yarns. It can be seen the fibers were well impregnated at loading of 40 wt% by PLA resin using the prepreg technology. As presented in Fig. 13c, the PLA matrix of NFPC between fiber bundles appears a typical brittle failure. The broken PLA mass disperses surrounding fibers. With incorporation of core–shell nanoparticle, the lamination of matrix between fiber bundles occurs, exhibiting a more ductile fracture (Fig. 13d). Excepting for the fibration effect induced by the core–shell filler, the shear yielding produced at the interface between fiber bundles and matrix also contributes to the exfoliation of PLA.

Conclusions

A designed rigid core–soft shell nanoparticle was introduced into the PLA matrix to strengthen the jute/PLA biocomposite meanwhile maintaining its ductility. The core–shell nanoparticle with both the rigid and rubbery phases was synthesized via chemical polymerization of nano-silica as the inner core and poly (butyl acrylate) as outer shell. The effect of core–shell filler on the crystalline, thermal and mechanical properties of NFPC was investigated. The WAXD results revealed that the core–shell nanofiller, as a nucleating agent, can promote the formation of complete crystalline grain of PLA. From the thermal analysis, the applied core–shell modifier is capable of improving the thermal stability of NFPC, and remaining its glass transition and melting temperatures as well. Furthermore, as the tensile and flexural tests presented, with the core–shell nanofiller

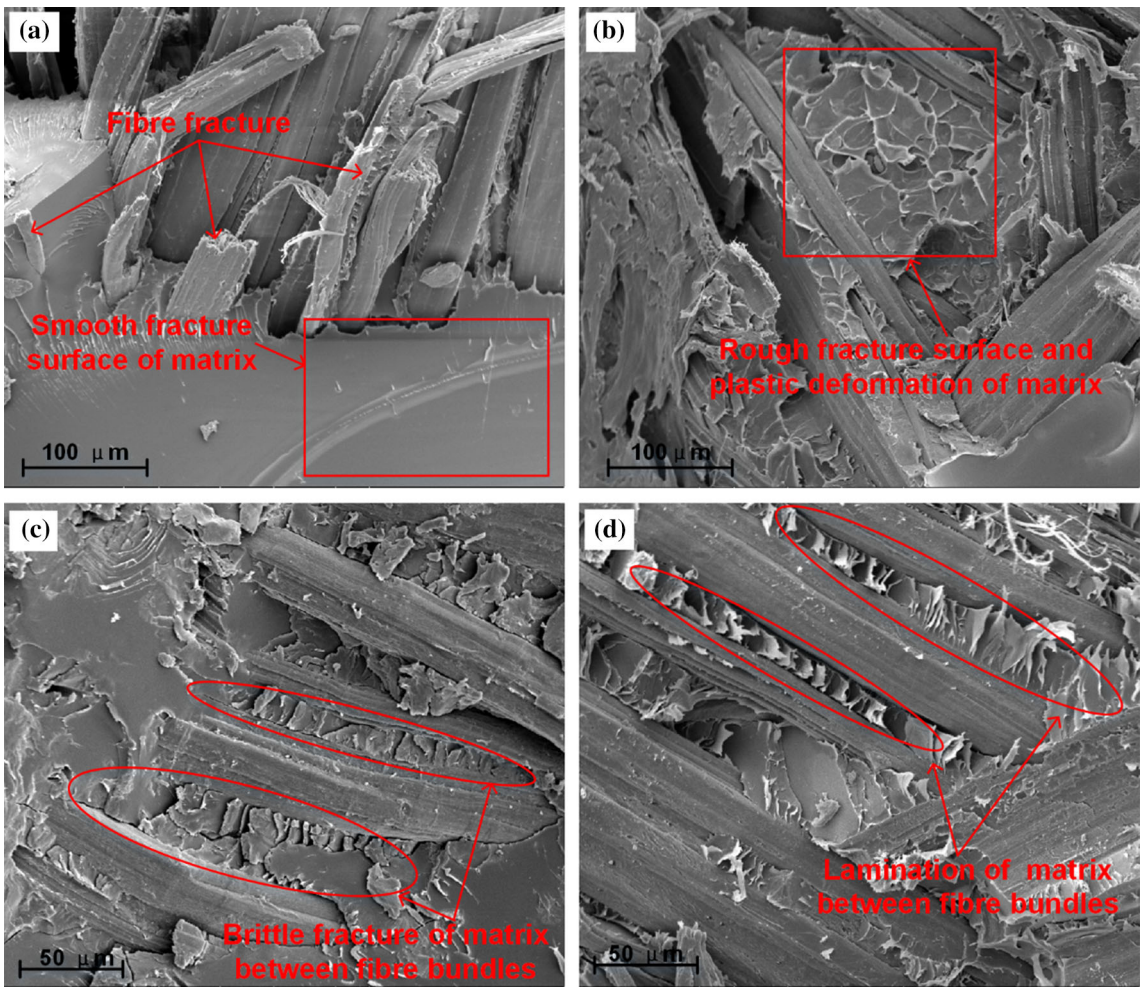

Figure 13 SEM fracture surface morphologies of PLA/jute fiber composites **a**, **c** NFPC; **b**, **d** NFPC/SiO_2–PBA–NH_2.

adding, the strength and stiffness of NFPC were significantly enhanced, especially, its toughness and elongation at break were not impaired. The superior mechanical properties are derived from the strong filler-matrix interactions and efficient synergy between rigid and rubbery phases of core–shell filler caused by the covalently bonding. Moreover, the fracture surface morphologies of PLA and NFPC revealed that the localized plastic deformation of matrix induced by core–shell filler is the main toughening mechanism.

Acknowledgements

This work was supported financially by the National Natural Science Foundation of China (Grant Nos. 11472086, 11532013 and 11872157). The author would like to gratefully acknowledge the China Scholarship Council that gives me a support to do research in the National University of Singapore.

References

[1] Pickering KL, Efendy MGA, Le TM (2016) A review of recent developments in natural fiber composites and their mechanical performance. Compos A Appl Sci Manuf 83:98–112

[2] Siengchin S (2017) Editorial corner—a personal view potential use of 'green' composites in automotive applications. eXPRESS Polym Lett 11:600

[3] Mavinkere S, Siengchin S (2018) Natural fibers as perspective materials. KMUTNB Int J Appl Sci Technol 11:233

[4] Qu P, Gao Y, Wu G, Zhang L (2010) Nanocomposites of poly (lactic acid) reinforced with cellulose nanofibrils. BioResources 5:1811–1823

[5] Bax B, Müssig J (2008) Impact and tensile properties of PLA/Cordenka and PLA/flax composites. Compos Sci Technol 68:1601–1607

[6] Pan P, Zhu B, Kai W, Serizawa S, Iji M, Inoue Y (2007) Crystallization behavior and mechanical properties of bio-based green composites based on poly (L-lactide) and kenaf fiber. J Appl Polym Sci 105:1511–1520

[7] Nishino T, Hirao K, Kotera M, Nakamae K, Inagaki H (2003) Kenaf reinforced biodegradable composite. Compos Sci Technol 63:1281–1286

[8] Yu T, Ren J, Li S, Yuan H, Li Y (2010) Effect of fiber surface-treatments on the properties of poly (lactic acid)/ramie composites. Compos A Appl Sci Manuf 41:499–505

[9] Goriparthi BK, Suman KNS, Rao NM (2012) Effect of fiber surface treatments on mechanical and abrasive wear performance of polylactide/jute composites. Compos A Appl Sci Manuf 43:1800–1808

[10] Huda MS, Drzal LT, Mohanty AK, Misra M (2008) Effect of fiber surface-treatments on the properties of laminated biocomposites from poly (lactic acid) (PLA) and kenaf fibers. Compos Sci Technol 68:424–432

[11] Kobayashi S, Takada K (2013) Processing of unidirectional hemp fiber reinforced composites with micro-braiding technique. Compos A Appl Sci Manuf 46:173–179

[12] Plackett D, Andersen TL, Pedersen WB, Nielsen L (2003) Biodegradable composites based on L-polylactide and jute fibres. Compos Sci Technol 63:1287–1296

[13] Kumar R, Yakabu MK, Anandjiwala RD (2010) Effect of montmorillonite clay on flax fabric reinforced poly lactic acid composites with amphiphilic additives. Compos A Appl Sci Manuf 41:1620–1627

[14] Thitsartarn W, Fan X, Sun Y, Yeo JCC, Yuan D, He C (2015) Simultaneous enhancement of strength and toughness of epoxy using POSS-Rubber core–shell nanoparticles. Compos Sci Technol 118:63–71

[15] Li Q, Zhang L, Zhang Z, Zhou N, Cheng Z, Zhu X (2010) Air-tolerantly surface-initiated AGET ATRP mediated by iron catalyst from silica nanoparticles. J Polym Sci Part A Polym Chem 48:2006–2015

[16] Ren Y, Zhou G, Cao P (2016) Preparations and properties of a tunable void with shell thickness SiO_2@SiO_2 core–shell structures via activators generated by electron transfer for atom transfer radical polymerization. Solid State Sci 52:154–162

[17] Zhan X, Yan Y, Zhang Q, Chen F (2014) A novel superhydrophobic hybrid nanocomposite material prepared by surface-initiated AGET ATRP and its anti-icing properties. J Mater Chem A 2:9390–9399

[18] Zafar MT, Maiti SN, Ghosh AK (2016) Effect of surface treatment of jute fibers on the interfacial adhesion in poly (lactic acid)/jute fiber biocomposites. Fibers and Polym 17:266–274

[19] Du Y, Wu T, Yan N, Kortschot MT, Farnood R (2014) Fabrication and characterization of fully biodegradable natural fiber-reinforced poly (lactic acid) composites. Compos B Eng 56:717–723

[20] Masirek R, Kulinski Z, Chionna D, Piorkowska E, Pracella M (2007) Composites of poly (L-lactide) with hemp fibers: morphology and thermal and mechanical properties. J Appl Polym Sci 105:255–268

[21] Lee BH, Kim HS, Lee S, Kim HJ, Dorgan JR (2009) Biocomposites of kenaf fibers in polylactide: role of improved

interfacial adhesion in the carding process. Compos Sci Technol 69:2573–2579

[22] Sawpan MA, Pickering KL, Fernyhough A (2011) Effect of fiber treatments on interfacial shear strength of hemp fiber reinforced polylactide and unsaturated polyester composites. Compos A Appl Sci Manuf 42:1189–1196

[23] Zhang J, Duan Y, Sato H, Tsuji H, Noda I, Yan S, Ozaki Y (2005) Crystal modifications and thermal behavior of poly (L-lactic acid) revealed by infrared spectroscopy. Macromolecules 38:8012–8021

[24] Liang JZ, Zhou L, Tang CY, Tsui CP (2013) Crystalline properties of poly (L-lactic acid) composites filled with nanometer calcium carbonate. Compos B Eng 45:1646–1650

[25] Nam JY, Sinha Ray S, Okamoto M (2003) Crystallization behavior and morphology of biodegradable polylactide/layered silicate nanocomposite. Macromolecules 36:7126–7131

[26] Dong Y, Ghataura A, Takagi H, Haroosh HJ, Nakagaito AN, Lau KT (2014) Polylactic acid (PLA) biocomposites reinforced with coir fibres: evaluation of mechanical performance and multifunctional properties. Compos A Appl Sci Manuf 63:76–84

[27] Adeli H, Hussein Sharif Zein S, Huat Tan S, Md Akil H, Latif Ahmad A (2011) Synthesis, characterization and biodegradation of novel poly (L-lactide)/multiwalled carbon nanotube porous scaffolds for tissue engineering applications. Curr Nanosci 7(3):323–332

[28] Kabir MM, Wang H, Lau KT, Cardona F, Aravinthan T (2012) Mechanical properties of chemically-treated hemp fiber reinforced sandwich composites. Compos B Eng 43:159–169

[29] Siengchin S, Pohl T, Medina L, Mitschang P (2013) Structure and properties of flax/polylactide/alumina nanocomposites. J Reinf Plast Compos 32:23–33

[30] Qin L, Qiu J, Liu M, Ding S (2011) Mechanical and thermal properties of poly (lactic acid) composites with rice straw fiber modified by poly (butyl acrylate). Chem Eng J 166:772–778

[31] Porras A, Maranon A (2012) Development and characterization of a laminate composite material from polylactic acid (PLA) and woven bamboo fabric. Compos B Eng 43:2782–2788

[32] Yang H, Li F, Shan C, Han D, Zhang Q, Niu L, Ivaska A (2009) Covalent functionalization of chemically converted graphene sheets via silane and its reinforcement. J Mater Chem 19:4632–4638

[33] Li X, Lei B, Lin Z, Huang L, Tan S, Cai X (2014) The utilization of bamboo charcoal enhances wood plastic composites with excellent mechanical and thermal properties. Mater Des 53:419–424

[34] He C, Donald AM, Butler MF (1998) In-situ deformation studies of rubber toughened poly (methyl methacrylate): influence of rubber particle concentration and rubber cross-linking density. Macromolecules 31:158–164

[35] Johnsen BB, Kinloch AJ, Mohammed RD, Taylor AC, Sprenger S (2007) Toughening mechanisms of nanoparticle-modified epoxy polymers. Polymer 48:530–541

[36] Yin B, Li LP, Zhou Y, Gong L, Yang MB, Xie BH (2013) Largely improved impact toughness of PA6/EPDM-*g*-MA/HDPE ternary blends: the role of core–shell particles formed in melt processing on preventing micro-crack propagation. Polymer 54:1938–1947